Available online at www.sciencedirect.com
SCIENCE DIRECT
Biosensors and Bioelectronics 21 (2006) 2255–2262
BIOSENSORS & BIOELECTRONICS
www.elsevier.com/locate/bios

Detection of *Escherichia coli* O157:H7 with langasite pure shear horizontal surface acoustic wave sensors

E. Berkenpas [a], P. Millard [b], M. Pereira da Cunha [a,*]

[a] *Department of Electrical and Computer Engineering, University of Maine, Orono, ME, USA*
[b] *Department of Chemical and Biological Engineering, University of Maine, Orono, ME, USA*

Received 9 July 2005; received in revised form 24 October 2005; accepted 8 November 2005
Available online 13 December 2005

Abstract

The toxigenic *Escherichia coli* O157:H7 bacterium has been connected with hemorrhagic colitis and hemolytic uremic syndrome, which may be characterized by diarrhea, kidney failure and death. On average, O157:H7 causes 73,000 illnesses, 2100 hospitalizations and 60 deaths annually in the United States alone. There is the need for sensors capable of rapidly detecting dangerous microbes in food and water supplies to limit the exposure of human and animal populations. Previous work by the authors used shear horizontal surface acoustic wave (SH SAW) devices fabricated on langasite (LGS) Euler angles (0°, 22°, 90°) to successfully detect macromolecular protein assemblies. The devices also demonstrated favorable temperature stability, biocompatibility and low attenuation in liquid environments, suggesting their applicability to bacterial detection. In this paper, a biosensor test setup utilizing a small volume fluid injection system, stable temperature control and high frequency phase measurement was applied to validate LGS SH SAW biosensors for bacterial detection. The LGS SH SAW delay lines were fabricated and derivatized with a rabbit polyclonal IgG antibody, which selectively binds to *E. coli* O157:H7, in this case a non-toxigenic test strain. To quantify the effect of non-specific binding (negative control), an antibody directed against the trinitrophenyl hapten (TNP) was used as a binding layer. Test *E. coli* bacteria were cultured, fixed with formaldehyde, stained with cell-permeant nucleic acid stain, suspended in phosphate buffered saline and applied to the antibody-coated sensing surfaces. The biosensor transmission coefficient phase was monitored using a network analyzer. Phase responses of about 14° were measured for the *E. coli* detection, as compared to 2° due to non-specific anti-TNP binding. A 30:1 preference for *E. coli* binding to the anti-O157:H7 layer when compared to the anti-TNP layer was observed with fluorescence microscopy, thus confirming the selectivity of the antibody surface to *E. coli*.

Keywords: SAW; Langasite; *E. coli*; Antibodies; Immunosensor

1. Introduction

Dissemination of harmful bacteria in food or water supplies as a result of accidents, pollution or terrorist activity can produce serious consequences in the form of economic losses and human suffering. Sensitive and selective sensors capable of rapidly and accurately detecting minute quantities of pathogens are urgently required. The need for real-time detection of biological and biochemical analytes is a major driving force behind the development of novel biosensor technology (Drell and Sofaer, 1999; Gizeli and Lowe, 2002; Su and Yanbin, 2004).

A pathogenic strain of the normally benign *E. coli* bacterium is the target of this work. The O157:H7 *Escherichia coli* (*E. coli*) bacterium has been linked to hemorrhagic colitis and hemolytic uremic syndrome (Rangel et al., 2005). These illnesses may cause diarrhea, kidney failure, seizure, stroke and death. Illness due to *E. coli* is often misdiagnosed and commonly results in invasive and expensive medical tests before it is correctly diagnosed. Primary sources for exposure to O157:H7 are ground beef, unpasteurized milk, fruit, vegetables and unchlorinated water (Rangel et al., 2005).

Traditional methods in use for detection of *E. coli* involve standard clinical microbiological assays which are characterized by long incubation times on the order of 24–72 h (Baron and Finegold, 1990; Ivnitski et al., 1999). These methods generally entail sample collection and incubation at a local healthcare facility followed by transfer of the prepared sample to a

* Corresponding author. Tel.: +1 207 5812384; fax: +1 207 5814531.
E-mail address: mdacunha@eece.maine.edu (M. Pereira da Cunha).

0956-5663/$ – see front matter © 2005 Elsevier B.V. All rights reserved.
doi:10.1016/j.bios.2005.11.005

centralized laboratory where apparatus and expertise for performing such tests have been concentrated. Tests for identification of pathogens often employ visual inspection with optical microscopy, flow cytometry, redox reactions, ultrasound techniques, gas phase chromatography, infrared spectroscopy and polymerase chain reaction (Ivnitski et al., 1999).

More recently biosensor techniques have been explored for microbial detection, in particular for use in the detection of pathogenic bacteria. Both indirect methods, which use labels or indirect methods as sensing mechanisms, and direct methods, which directly detect the target measurands, are under intense research and development (Ivnitski et al., 1999; Abdel-Hamid et al., 1999; Ruan et al., 2003). For instance, indirect methods are those which rely on the use of fluorescence labels, microbial metabolism, magnetoelastic immunosensors and electrochemical immunodetection. Examples of direct methods are: optical detection, bioluminescence, impedance measurement and acoustic wave detection for direct measurement of a physical property change due to an analyte (Ivnitski et al., 1999; Gizeli and Lowe, 2002). While indirect methods provide good sensitivity, direct methods are an alternative to indirect methods, which allow label-free detection of cells and tissues and therefore decrease the measurement complexity.

Examples of acoustic wave bacterial sensor platforms mentioned in the literature involve the use of commercially available quartz crystal microbalance (QCM) devices, which operate based on bulk acoustic wave resonation between smooth surfaces of a thin, piezoelectric, quartz wafer (Suleiman and Guilbault, 1994; Ivnitski et al., 1999; Deisingh and Thompson, 2002; Su and Yanbin, 2004). The thickness shear mode (TSM) on AT cut quartz is utilized in most QCM biosensors for mass detection, due to the low attenuation the mode exhibits in the presence of liquids.

Surface acoustic wave (SAW) devices are an alternative acoustic wave platform to the QCM, with the possibility of integration into array systems due to miniaturization, and potential increased sensitivity due to the surface guided nature of the wave and a higher operating frequency (Ballantine et al., 1997; Freudenberg et al., 2001; Gizeli and Lowe, 2002). These devices can be fabricated inexpensively in large quantities, utilizing single-step photolithographic processes, widely used in the semiconductor industry. The SAW devices can be configured as resonators or delay lines, with the maximum operating frequency constrained by the minimum achievable line-width of the photolithographic process, given a SAW velocity for a specific material and propagation direction.

For a SAW device to operate as a biosensor platform in liquid phase, the shear horizontal (SH) SAW mode is selected. Rayleigh or general polarized SAW modes excite longitudinal waves in the liquid, which results in significant SAW device losses (>40 dB), unusable in liquid media and therefore impractical as a biosensor (Calabrese et al., 1987; Kondoh and Shiokawa, 1993; Andle and Vetelino, 1995; Pereira da Cunha et al., 2002).

Three different techniques are listed in the literature for the detection of bacteria using bulk and surface acoustic wave devices: flow-through, dip-and-dry and immersion (Cunningham, 1998; Ivnitski et al., 1999; Gizeli and Lowe, 2002; Su and Yanbin, 2004). In flow-through experiments, bacteria in a buffer solution are allowed to flow over the sensing surface. In the dip-and-dry tests, the detecting surface is dried after it has been exposed to the bacteria. By allowing attached bacteria to dry onto the sensing surface, mechanical coupling between the sensor and the analyte bacteria is increased, which is advantageous in increasing the device's sensitivity. Finally, in immersion tests, the entire sensor device is immersed in a buffer solution to establish a baseline response, followed by submersion in the suspension of the target analyte bacteria.

SH SAW devices using quartz (Howe and Geoffrey, 2000) and pseudo-SAW (PSAW) devices using $LiTaO_3$ (Su and Yanbin, 2004) have been employed as immunosensors for bacterial detection. The SH SAW mode on quartz suffers from low electromechanical coupling coefficients, high penetration depth, and low dielectric permittivity with respect to the liquid media. The PSAW mode on $LiTaO_3$ suffers from extra attenuation in liquids due to the intrinsic associated vertical particle displacement component, and the attenuation of the acoustic wave due to the excitation of the BAW mode into the bulk of the crystal.

The langasite family of crystals (LGX), which includes langasite (LGS, $La_3Ga_5SiO_{14}$), langanite (LGN, $La_3Ga_{5.5}Nb_{0.5}O_{14}$) and langatate (LGT, $La_3Ga_{5.5}Ta_{0.5}O_{14}$), has been suggested as a possible alternative for SAW devices operating in liquids (Pereira da Cunha et al., 2002). Among the promising characteristics of these crystals applicable to liquid sensing, one can list: (i) the existence of pure SH guided SAW modes along Euler angles (0°, θ, 90°); (ii) a shallow acoustic penetration depth, in which most of the energy in the wave is concentrated at the surface, thus favoring sensitive SH SAW sensor response; (iii) the existence of SH SAW orientations with electromechanical coupling up to 10 times higher than the equivalent SH SAW 35.8°-Y rotated quartz, along Euler angles (0°, −54.2°, 90°); (iv) the occurrence of zero temperature coefficient of delay (TCD) for the SH SAW modes; (v) high values of dielectric permittivity, further confining the electrical fields in the piezoelectric crystal and thus improving transduction of the wave in the presence of high dielectric media such as water and (vi) a low SH SAW phase velocity, 50% below that of 35.8° Y rotated quartz, which favors smaller sensors.

Experimental SH SAW devices have been designed, fabricated, and tested along LGT and LGS orientations in (Pereira da Cunha et al., 2002) and (Berkenpas et al., 2004), verifying the properties previously listed and the suitability of LGS for operation in liquids. LGS operation along the propagation direction Euler angles (0°, 22°, 90°) presents (Berkenpas et al., 2004): (1) relatively strong piezoelectric coupling (0.4%); (2) reduced additional attenuation (6 dB) due to liquid loading or lossy material, such as liquid chamber rubber, at the surface; (3) reduced temperature dependence, with zero temperature coefficient of frequency (TCF) or turn over temperature identified at 20 °C, and a fractional frequency variation, $\Delta f/f_o$, of 2.5 ppm over 5 °C around the turn over temperature and (4) suitability for biological detection, indicated by the fabricated and flow-through tested LGS SH SAW devices, which produced measurable transmission phase variations due to antibody binding on the sensor surface.

This paper reports the original and successful use of the SH SAW mode on LGS as a bacteria sensor. The design, fabrication and testing of an LGS SH SAW delay line applied to *E. coli* bacterial detection is discussed, including the biofilm fabrication, the testing chamber, and test set up implemented. Immobilized antibodies (anti-O157:H7) have been used as sensing layers. The selective adhesion of *E. coli* to the anti-O157:H7 receptor surface was verified by exposing selective (anti-O157:H7) and non-selective surface control surface (anti-*trinitrophenol*, or anti-TNP) to fluorescently labeled *E. coli* to allow a comparison between the numbers of bound bacteria. Langasite delay line platforms designed and fabricated along the propagation direction Euler angles (0°, 22°, 90°) have been tested using both flow-through and dip-and-dry detection techniques. The tests performed with a dip-and-dry technique show a consistent sensor response to *E. coli* detection of about 14° variation in the phase of the transmission coefficient, $\angle S_{21}$, whereas the tests with the flow-through method indicate reduced 0.7° variation of $\angle S_{21}$. This result is discussed in light of the penetration depth of shear particle displacement inside the liquid media. A successful methodology for surface preparation of gold metalized LGS substrates for the detection of *E. coli* using LGS SH SAW devices has been achieved, as verified by the repetitive and consistent LGS SH SAW tests reported in this work. Section 2 describes the fabrication of the SH SAW device; the assembly of the biological sensing layer; the implementation of the test set up; and the methodology used to verify the LGS SH SAW bacterial immunosensor operation. Section 3 presents and discusses the results obtained. Section 4 concludes the paper.

2. Materials and methods

2.1. Fabrication of the SH SAW LGS devices

The LGS SH SAW bacterial immunosensor delay lines (Fig. 1) designed and fabricated in this work along propagation direction Euler Angles (0°, 22°, 90°) used gold thin film as electrodes for SH SAW excitation and as a platform for the assembly of the protein immobilization layer. The metallic layer consisted of a 600 Å sputtered layer of gold (Au) on top of a 100 Å chromium (Cr) adhesion layer. It should be noted that the gold film was found to have excellent adhesion to the LGS substrate. No delamination of the gold film was observed during fabrication or testing. Conventional microelectronic photolithographic and wet-etch techniques were employed to pattern the interdigital transducers (IDTs) and the gold platform region upon which

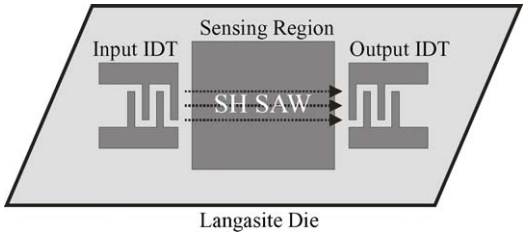

Fig. 1. A diagram of the LGS SH SAW sensor.

the antibody immobilization layer was assembled. The metallic layer in the delay path also served to electrically shield the SH SAW from unwanted variations in liquid conductivity. Each IDT consists of 240 electrodes, arranged in split-finger configuration to minimize overall transducer reflection; with an electrode width of 4 μm; metalization ratio 0.5; thus IDT periodicity of 32 μm and acoustic aperture equal to 1600 μm. To additionally limit interference due to acoustic reflections from the border of the device, the die edges were angled, as represented in Fig. 1.

2.2. Assembly and tests of the biolochemical sensing layer

An antibody (anti-O157:H7 or anti-*E. coli*) layer assembly was used in this work for specific bacterial adhesion to the LGS SH SAW sensor delay. Mercaptoethylamine (cysteamine) diluted in ethanol was initially applied to a gold sensing surface for 12 h at 10 °C to produce an amine monolayer. The surface was then rinsed sequentially with ethanol and water, and then dried with argon. In the next step, the surface was exposed to *N*-hydroxysuccinide poly(ethylene glycol)-5000 biotin (NHS-PEG-biotin, PT-11D-34 Etkar) in phosphate buffered saline (PBS). NHS-PEG-biotin was then reacted with free amine groups on to the cysteamine surface, and the surface rinsed with 10 mM glycine. In order to fill free binding sites, thus blocking non-specific binding of subsequent molecular components, the surface was rinsed with bovine serum albumin (BSA) in PBS. NeutrAvidin™ was bound to biotin groups attached to the sensor surface. A biotinylated polyclonal rabbit immunoglobulin G (IgG) antibody directed against *E. coli* was then attached to surface bound NeutrAvidin™, followed by a BSA buffer rinse to yield the completed antibody sensing layer.

An enzyme-linked immunosorbent assay (ELISA) method was employed to verify the correct assembly of the protein layer (Molecular Probes, 2003). Gold layered surfaces on glass slides were prepared with rabbit IgG antibodies following the procedure previously described. Goat anti-rabbit IgG labeled with horseradish peroxidase (HRP) were used to selectively attach to surfaces containing rabbit IgG antibodies. Amplex Red and hydrogen peroxide (H_2O_2) were added to the labeled surface. The HRP enzyme catalyzes a reaction of Amplex Red and H_2O_2 into resorufin, a detectable fluorescent product measured with an A153600 Fusion Universal microplate reader (Perkin-Elmer, Inc., Wellesly, MA). Surfaces without NeutrAvidin™ and surfaces without NHS-PEG-biotin, NeutrAvidin™, and rabbit anti-O157:H7 served as negative controls. Background flourescence was determined by measuring resorufin fluorescence in Amplex Red and H_2O_2 solution without HRP.

In order to verify the selective adhesion of *E. coli* to the anti-O157:H7 receptor surface and to compare specific and non-specific binding, bacteria labeled with SYTO-9 nucleic acid stain (Molecular Probes, Inc., Eugene, OR) were applied to both an anti-O157:H7 surface and to an anti-TNP control surface. In this test, *E. coli* was streaked onto a nutrient agar plate and grown overnight at 37 °C. A test tube of nutrient broth was inoculated with a single colony and incubated for 4 h in a G24 incubator-shaker (New Brunswick Scientific, Edison, NJ) at 37 °C and

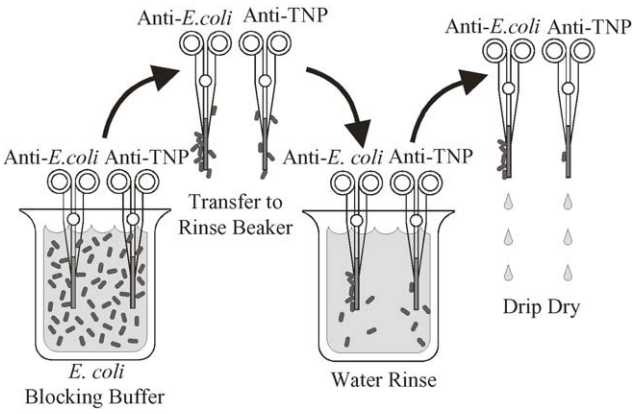

Fig. 2. Experiments to quantify adhesion and non-specific binding using gold plated glass slides with anti-O157:H7 and anti-TNP (control slide) prepared surfaces.

250 rpm. Growth was confirmed by observation of turbidity and a 250 mL flask was inoculated with the culture and incubated in a G24 incubator-shaker for 7 h. The nutrient broth containing live *E. coli* was centrifuged at 4100 × *g* for 40 min with an Allegra^{TM} 21R Centrifuge (Beckman Coulter, Fullerton, CA) and resuspended four times in PBS. The rinsed *E. coli* were fixed with formaldehyde, washed two times by centrifuge and resuspended in BSA PBS. Glass slides were magnetron-sputtered with 100 Å of chromium and 2000 Å of gold. The gold surfaces were prepared for anti-O157:H7 and anti-TNP (control slide) as previously described. The slides were then immersed in a 500 mL beaker filled with *E. coli* ($\sim 10^9$ cells/mL) in PBS BSA for gently stirred with a magnetic stir bar for 5 h (Fig. 2). The slides were transferred to a rinse beaker, where loosely bound bacteria were allowed to disassociate from the surface for 5 h. The slides were then removed from the water, allowed to dry for 2 h, and imaged by fluorescence microscopy with a cooled CCD camera (Spot-2, Diagnostic Instruments, Sterling Heights, MI) on a BX51 fluorescence microscope (Olympus). Finally, a cell counting algorithm (Metamorph v6.2r4, Universal Imaging Corp., Downingtown, PA) was utilized to compare selective binding *E. coli* to the anti-O157:H7 slide versus non-selective binding to the anti-TNP slide as visualized in the digital images.

2.3. Measurement setup and test procedure for E. coli flow-through experiments

Fig. 3 shows the experimental setup for flow-through tests of LGS SH SAW sensors in fluids. LabVIEW^{TM} 6i platform (National Instruments Corp., Austin, TX) installed in a personal computer was used to control a syringe pump, a control valve and an HP 4195A network analyzer. The computer controlled Micro4^{TM} syringe pump (World Precision Instruments, Inc., Sarasota, FL) dispensed fluids at regulated flow rates through 150 μm inside diameter capillary tubing to a V-445 actuated, low dead volume rotary valve (Upchurch Scientific, Inc., Oak Harbor, WA). The valve enabled purging of air bubbles from the tubing. Stainless steel tubing coupled to the capillary tubing, was modified to fit with a custom designed laser-cut plastic flow cell (Grace Biolabs, Inc., Bend, OR) aligned over the LGS SH SAW delay path. Fluids flowing through the chamber were channeled via a second stainless steel insertion tube to a waste beaker.

Also shown in Fig. 3 is a CZ1 solid-state Peltier device (Tellurex Corp., Traverse City, MI) used to control the LGS SH SAW sensor temperature. The Peltier device is sandwiched between an aluminum thermal mass and a heat sink. The LGS SH SAW sensor was mounted on the other side of the aluminum thermal mass with double sided scotch tape (3M). An F3107 platinum resistance temperature device (RTD, Omega Engineering Inc., Samford, CT) in thermal contact with the LGS SH SAW sensor provided temperature feedback to a standard CNi series digital temperature controller (Omega) used in conjunction with a specially designed driver circuit to supply the correct voltage and current to the Peltier device. Temperature was maintained by pumping heat to and from the sensor to ambient air. The test setup allowed consistent temperature control within ±0.1 °C

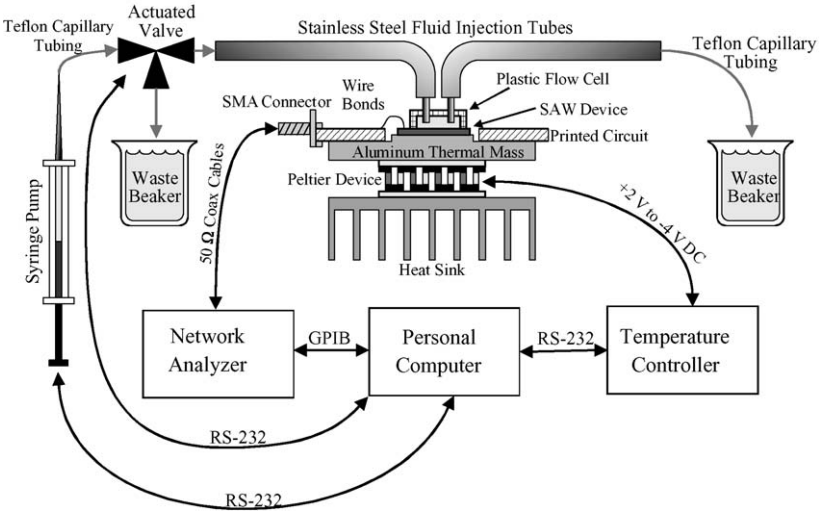

Fig. 3. Experimental set up for flow-through tests.

over a range of 10–35 °C. For all tests reported in this work the temperature was set to 25 °C.

The LGS SH SAW sensor was wire bonded to a custom designed copper clad printed circuit board containing 50Ω microstrip transmission lines which were soldered to edge-launch coaxial subminiature type-A (SMA) connectors (Pasternack Enterprises, Irvine, CA). The HP 4195A network analyzer (Agilent Technologies, Inc., Palo Alto, CA) was connected to the SMA connectors through RG58C/U 50Ω coaxial cables (Pasternack Enterprises, Irvine, CA). A custom LabVIEW routine was written to record the magnitude and phase of the transmission coefficient (S_{21}) sensor response at the fixed frequency of 92 MHz, in the neighborhood of the center frequency, as a function of time. The LabVIEW routine was also used to set and record the LGS SH SAW sensor temperature via the temperature controller to control the syringe pump and to set the position of the actuated valve.

The *E. coli* selective antibody layer was assembled on the LGS SAW sensor delay-path as described in Section 2.2. Glycine or BSA rinse steps were performed over the sensing surface at 1.5 μL/s for 10 min. A solution of NHS-PEG-biotin (10 μM) was flowed into the liquid flow-cell at 60 nL/s for 2 h. NeutrAvidin™ (3 μM) and the biotinylated antibody (1.3 μM) were each allowed to flow into the liquid flow-cell at 120 nL/s for 1 h.

After the constituent molecules were applied to the sensing surface, PBS BSA was infused through the chamber for 2.5 h at 50 nL/s to establish a baseline for the transmission coefficient phase, $\angle S_{21}$. *E. coli* suspensions (~10^9 cells/mL) were prepared as described in Section 2.2 and allowed to flow over the sensor surface at 50 nL/s for 2.5 h. A stable $\angle S_{21}$ response was established by flowing water over the surface at 50 nL/s for 2.5 h. The sensor response was then given by the $\angle S_{21}$ change between the baseline and the response after *E. coli* suspension passed through the liquid flow-cell. The sensor was subsequently unmounted and imaged by fluorescence microscopy to quantify bacterial binding.

2.4. Measurement setup and test procedure for E. coli "dip-and-dry" experiments

Fig. 4 depicts the experimental setup used in this work for the dip-and-dry method of detecting bacteria. As in the previously described flow-through test setup, the personal computer-based LabVIEW™ 6i platform was used to control temperature and the network analyzer. All measurements were performed at 25 °C. Temperature control, network analyzer and data acquisition procedures were identical to those used in the flow-through tests.

Solutions containing analytes were dispensed into a 2 mm diameter silicone rubber fluid well aligned over the delaypath of the SAW sensing area using a volume-calibrated dispensing pipetter (Thermo Electron Corp., San Jose, CA). Placement of a microscope coverslip over the rubber sensing well limited evaporation.

The same antibody layer assembly described in Section 2.2 was used for the dip-and-dry experiments. The initial dry phase

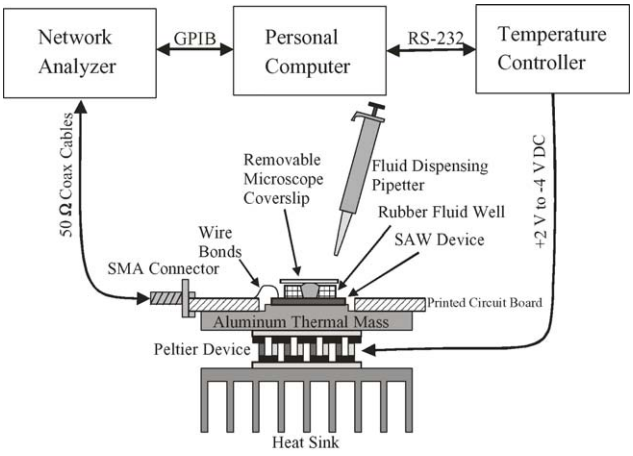

Fig. 4. Experimental set up for dip-and-dry tests.

sensor baseline was established for 1 h. NHS-PEG-biotin in PBS was added to the well and allowed to react with the sensor surface for another period of 1 h. Solutions were added and removed from the fluid well in 30 μL increment repetitions using the fluid pipetter. Glycine and BSA rinsing steps were performed 10 times. NeutrAvidin™ and the biotinylated antibody were each allowed to bind in the well for 30 min.

The prepared *E. coli* bacteria suspended in BSA (~10^9 cells/mL) were applied to the well and allowed to settle for 2 h under the coverslip. A final water rinse was performed five times to remove loosely bound *E. coli* from the surface and, at this point, the coverslip was not replaced, allowing the surface to dry. A final dry-phase $\angle S_{21}$ was established and measured. The $\angle S_{21}$ variation between an initial dry state of the LGS SH SAW sensor and a second dry state after the surface was prepared established the sensor response for this method. The devices were then unmounted and imaged with the microscope to quantify the number of bacteria bound to the surface.

3. Results and discussion

3.1. Surface preparation and bacterial adhesion to surfaces using antibodies

The ELISA procedure described in Section 2 was used to verify the correct assembly of the antibody protein layer on the surface of the gold-coated microscope slides. Two types of negative control surfaces were tested, the first without NeutrAvidin™ and the second without NHS-PEG-biotin, NeutrAvidin™ and rabbit anti-O157:H7. These negative controls produced levels of fluorescent product comparable to the background level, as measured by the spontaneous reaction of Amplex Red with H_2O_2 in the absence HRP. When the background level is subtracted antibody-assembled surfaces generated relative fluorescence levels 24 times greater than that seen on negative control surfaces, thus indicating the appropriate assembly of the sensing layer.

Anti-O157:H7 surfaces and anti-TNP control surfaces were assembled on gold-coated microscope slides according to the procedure described in Section 2, and used to verify selectivity

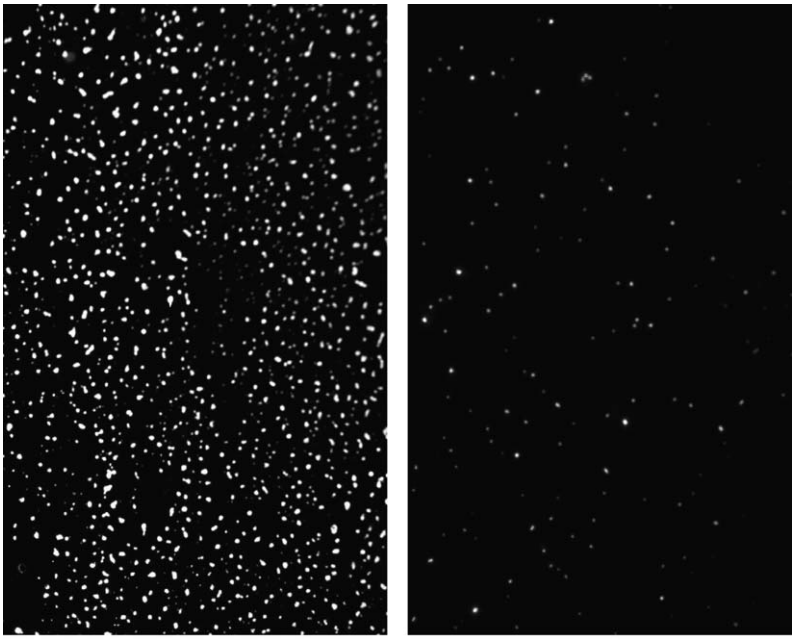

Fig. 5. Aggregates of fluorescently labeled *Escherichia coli* bacteria: (left) surface coated with antibodies directed against *E. coli* O157:H7 and (right) antibodies directed against TNP.

to *E. coli* bacteria. Fig. 5 shows images of fluorescently labeled *E. coli* on antibody-immobilized gold slides and on an anti-TNP control surface. The white dots on the image indicate aggregates of 20 or more *E. coli* bacteria formed when the surfaces were dried. Dark regions indicate areas of low binding. The Metamorph v6.2r4 image processing algorithm referred to in Section 2 was used to quantify the amount of specific and non-specific binding on the respective surfaces. A 30 times greater density of *E. coli* was bound to the anti-O157:H7 surface when compared to the slide prepared with immobilized anti-TNP, indicating the selectivity of the anti-O157:H7 layer assembly for *E. coli* detection.

3.2. SH SAW sensor response to bacteria in flow-through testing

The tests reported in this section refer to the LGS SH SAW flow-through test set up (Fig. 3). Fluorescence microscopy tests on the SH SAW substrate indicated 10 times greater *E. coli* bound onto the anti-O157:H7 surface with respect to the amount of binding measured on anti-TNP prepared surfaces. This result demonstrated that the antibody sensing surface was functioning as predicted under constant flow conditions.

A baseline for the LGS SH SAW $\angle S_{21}$ response was measured before the infusion of the *E. coli* suspension. The stable phase response after the infusion *E. coli* was then compared to the initial $\angle S_{21}$ baseline, resulting in $\angle S_{21}$ from 0.1 to 0.7° between experiments, which is comparable to the 0.3° typical $\angle S_{21}$ drift observed during experiments. In addition, the $\angle S_{21}$ responses obtained with the anti-O157:H7 surface were similar to those obtained with the anti-TNP control surfaces, which indicated negligible response to *E. coli* in liquids.

The low response in liquids is most likely due to low mechanical coupling between the bacteria and the sensing surface. The viscous decay length, δ, (Ballantine et al., 1997; Gizeli and Lowe, 2002) is used to represent the depth in the liquid where the shear wave fields of planar BAW incident to the surface are attenuated to $1/e$ (37%) of their surface values. The viscous decay length arises from fluidic equations governing laminar flow over smooth surfaces (White, 1991) and is described by the following expression (Ballantine et al., 1997; Gizeli and Lowe, 2002):

$$\delta = \sqrt{\frac{2\eta}{\omega\rho}} \tag{1}$$

where η is the liquid viscosity, ω the angular frequency of the sensor surface and ρ is the liquid density. If analytes exist beyond the viscous decay length they will not effectively couple to the surface and the detection or sensing mechanism is compromised.

In this particular experiment, (where $\eta = 0.89 \times 10^{-3}$ Pa s, $\omega = 2\pi 92 \times 10^6$ rad/s, and $\rho = 997.04$ kg/m^3) the viscous decay length into the liquid is approximately 560 Å. The *E. coli* attached to the surface is estimated to be around 800 Å above the surface, leaving it beyond the viscous decay length and compromising detection in flow-through testing.

3.3. SAW response to bacteria in dip-and-dry testing

A raw data phase curve versus time for six dip-and-dry tests is shown in Fig. 6. The solid curves show tests using anti-O157:H7 prepared surfaces. The dashed curves show experiments done with the anti-TNP negative control surface. An initial relative

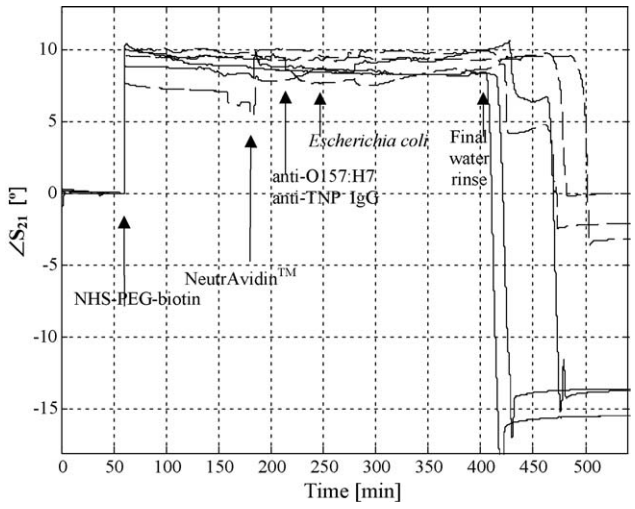

Fig. 6. LGS SH SAW sensor $\angle S_{21}$ response vs. time for multiple experiments. The solid lines indicate three experiments with *E. coli* and an anti-O157:H7 surface. The dashed lines indicate three experiments with *E. coli* and an anti-TNP surface.

phase baseline of 0° is established and at 60 min NHS-PEG-biotin is applied, causing an 8–11° increase in $\angle S_{21}$ over the dry surface. The phase remained between 5 and 10° above dry baseline for the next 350 min, during which time NeutrAvidin™, biotinylated anti-O157:H7 or biotinylated anti-TNP, and *E. coli* bacteria were applied to the fluid well. Phase variations over this time period were spurious and most likely caused by bubble formation, temperature variations and pressure variations on the surface, which resulted from the application and removal of solutions to the fluid well, as well as slow evaporation under the microscope coverslip. At between 400 and 500 min the phase decreased after the fluid well was rinsed five times with water and removed, allowing the surface to dry. Drying time varied between 20 and 70 min due to the variation in the amount in liquid left in the fluid well after the water rinse. The device response in this experiment consisted of two steps: first the bacteria were allowed to interact with the surface for about 2.5 h, and second, the fluid was allowed to dry, as previously indicated. This work did not focus on the optimization of the dip-and-dry method response time, which should be addressed in a future effort. Decrease in phase indicates a decrease in SH SAW velocity. Dried *E. coli*, bound to the sensing region, increases surface mass and slows the SH SAW wave, creating a downward phase shift.

In all experiments, $\angle S_{21}$ was observed to increase slightly after an initial drop, and as *E. coli* further dried onto the sensor surface. This observation is thought to be due to *E. coli* dehydration at a slower rate than liquid evaporation at the surface. The *E. coli* dehydration decreases their mass, therefore decreasing the overall mass at the sensor surface, causing a slight recovery of the phase response. The suggested explanation for the $\angle S_{21}$ response seems to be confirmed by the larger phase variations observed when larger amounts of surface bound *E. coli* are present. Fig. 6 shows that a consistent phase difference, larger than 10°, has been measured between the selective anti-O157:H7 response and the non-selective anti-TNP response.

Numerical calculations using Adler's matrix method (Adler, 1994) and experimental results for mass and viscosity sensitivity recently reported (Berkenpas et al., in press) show that the mass and viscosity sensitivity of the device under liquid operation to be about −2550 (ppm m^2/g) and −8.61 ppm/(mPa s), respectively. These numbers are comparable to the pseudo SAW mode on $LiTaO_3$, a crystal that has been recently used in SAW biosensor research (Kondoh and Shiokawa, 1993). The estimated sensitivity for the LGS SH SAW biosensor results reported in this paper is 10° for 10^9 *E. coli* bacteria/ml, assuming an approximated linear response. Based on a measured $\angle S_{21}$ noise of 0.05°, the limit of detection (LOD) can be approximated at $\sim 10^6$ cells/ml, which is comparable to LODs of acoustic wave sensors found in literature (Huramatsu et al., 1986; Ivnitski et al., 1999; Pathirana et al., 2000; Su and Yanbin, 2004). Future work on the LGS SH SAW biosensor shall aim at improving the sensitivity of the device by optimizing both bioreceptive layer and the LGS SH SAW platform modeling and design.

4. Conclusions

LGS SH SAW biosensors were designed, fabricated and tested. Surface chemistry and selective binding of bacteria was verified. Two experimental methods were used: a liquid phase flow-through method and a dip-and-dry method. The flow-through method produced reduced (0.1–0.7°) variation in the $\angle S_{21}$ response, credited to the relatively large distance of the *E. coli* from the sensitive LGS SH SAW surface with respect to the viscous decay length.

For the dip-and-dry method, where the *E. coli* was selectively bound and then dried onto the surface of the LGS SH SAW delay line, a significant and measurable variation of the $\angle S_{21}$ response was produced (13.5–15.5°). The same measurement for *E. coli* exposed to anti-TNP prepared surfaces resulted in variations of $\angle S_{21}$ between 0 and 3°, indicating a phase difference larger than 10° between the selective anti-O157:H7 response and the non-selective anti-TNP response. This significant and reproducible LGS SH SAW sensor response confirmed the viability of the device as a selective *E. coli* detector, with potential for further development into an inexpensive portable detector for *E. coli* O157:H7.

Acknowledgement

This work was conducted with support from the National Science Foundation (grants ECS-0233463, ECS-0329913, and DGE-0139324).

References

Abdel-Hamid, I., Ivnitski, D., Atanasov, P., Wilkins, E., 1999. Flow-through immunofiltration assay system for rapid detection of *E. coli* O157:H7. Biosens. Bioelectron. 14, 309–316.

Adler, E., 1994. SAW and pseudo-SAW properties using matrix methods. IEEE Trans. Ultrasonics, Ferroelect. Frequency Control 41 (November (6)), 876–882.

Andle, J.C., Vetelino, J.F., 1995. Acoustic wave sensors. In: Proceedings of the 1995 IEEE Ultrasonics Symposium, pp. 451–460.

Ballantine, D.S., White, R.M., Martin, S.J., Ricco, A.J., Zellers, E.T., Frye, G.C., Wohltjen, H.W., 1997. Acoustic Wave Sensors: Theory, Design and Physico-Chemical Applications. Academic Press, London.

Baron, E., Finegold, S., 1990. Bailey & Scott's Diagnostic Microbiology, eighth ed. Mosby, St. Louis.

Berkenpas, E., Bitla, S., Millard, P., Pereira da Cunha, M., 2004. Pure Shear Horizontal SAW Biosensor on Langasite. IEEE Trans. Ultrasonics, Ferroelectr. Frequency Control 51, 1404–1411.

Berkenpas, E., Kenny, T., Millard, P., Pereira da Cunha, M. A Langasite SH SAW O157:H7 *E. coli* Sensor, Proceedings of the 2005 IEEE Ultrasonics Symposium, in press.

Calabrese, G., Wohltjen, H., Roy, M., 1987. Surface acoustic wave devices as chemical sensors in liquids: evidence disputing the importance of Rayleigh wave propagation. Anal. Chem. 59, 833–837.

Cunningham, A., 1998. Introduction to Bioanalytical Sensors. John Wiley & Sons.

Deisingh, A.K., Thompson, M., 2002. Detection of infectious and toxigenic bacteria. Analyst 127, 567–581.

Drell, S., Sofaer, A., 1999. The New Terror. Hoover Institution Press Publication, USA.

Freudenberg, J., Von Schickfus, M., Hunklinger, S., 2001. A SAW immunosensor for operation in liquid using a SiO_2 protective layer. Sens. Actuators B 71, 147–151.

Gizeli, E., Lowe, C.R., 2002. Biomolecular Sensors. Taylor & Francis, New York.

Howe, E., Geoffrey, H., 2000. A comparison of protocols for the optimization of detection of bacteria using a surface acoustic wave (SAW) biosensor. Biosens. Bioelectron. 15, 641–649.

Huramatsu, H., Kajiwara, K., Tamiya, E., Karube, I., 1986. Piezoelectric immunosensor for the detection of *Candida albicans* microbes. Anal. Chim. Acta 188, 257–261.

Ivnitski, D., Abel-Hamid, I., Atanasov, P., Wilkins, E., 1999. Biosensors for detection of pathogenic bacteria. Biosens. Bioelectron. 14, 599–624.

Kondoh, J., Shiokawa, S., 1993. A liquid sensor based on a shear horizontal SAW device. Electron. Commun. Jpn. 76 (2), 69–82, Part 2.

Molecular Probes, 2003. Amplex Red Hydrogen Peroxide/Peroxidase Assay Kit. http://probes.invitrogen.com/media/pis/mp22188.pdf.

Pathirana, S.T., Barbaree, J., Chin, B.A., Hartell, M.G., Neely, W.C., Vodyanoy, V., 2000. Rapid and sensitive biosensor for *Salmonella*. Biosens. Bioelectron. 15, 135–141.

Pereira da Cunha, M., Malocha, D.C., Puccio, R., Thiele, J., Pollard, T., 2002. LGX pure shear horizontal SAW for liquid sensor applications. IEEE Sens. J. 3, 554–561.

Rangel J.M., Sparling, P.H., Crowe, C., Griffin, P.M., Swerdlow, D.L., 2005. Epidemiology of *Escherichia coli* O157:H7 outbreaks, United States, 1982–2002, Emerg. Infect. Dis., www.cdc.gov 11(4).

Ruan, C., Zeng, K., Varghese, O., Grimes, C., 2003. Magnetoelastic immunosensors: amplified mass immunosorbent assay for detection of *Escherichia coli* O157:H7. Anal. Chem. 75, 6494–6498.

Su, X., Yanbin, Li, 2004. A self-assembled monolayer-based piezoelectric immunosensor for rapid detection of *Escherichia coli* O157:H7. Biosens. Bioelectron. 19, 563–574.

Suleiman, A.A., Guilbault, G.G., 1994. Recent developments in piezoelectric immunosensors. Analyst 119, 2279–2282.

White, F.M., 1991. Viscous Fluid Flow: Second Edition. McGraw Hill Inc., New York.